Reversible electromechanical characteristics of individual multiwall carbon nanotubes

V. Semet, Vu Thien Binh,[a] and D. Guillot
Equipe Emission Electronique, LPMCN-CNRS, Université Claude Bernard Lyon 1, Villeurbanne 69622, France

K. B. K. Teo, M. Chhowalla, G. A. J. Amaratunga, and W. I. Milne
Department of Engineering, University of Cambridge, Cambridge CB2 1PZ, United Kingdom

P. Legagneux and D. Pribat[b]
Thalès R&T France, Domaine de Corbeville, Orsay 91404, France

(Received 25 February 2005; accepted 27 September 2005; published online 21 November 2005)

Here we report the reversible change in the nonlinear conductance of a multiwall carbon nanotube (MWNT) when it is bent longitudinally. As the nanotube is compressed and bent, its resistance decreases dramatically. This behavior is fully recoverable. The observed drop in resistance during bending must be the result of increasing number of conduction channels in the nanotube and parallel transport through them. Using this concept of parallel transport, we show that it is indeed possible to electrically model the behavior of the MWNT under compression. The reversible electrical characteristics of a MWNT under bending opens new possibilities for these structures to be applied as nanoscale displacement sensors. © *2005 American Institute of Physics*.
[DOI: 10.1063/1.2136229]

Electrical transport in carbon nanotubes has been the subject of intense study over recent years. Many interesting phenomena have been discovered in both single wall and multiwall nanotubes, such as ballistic transport,[1] spin coherent transport,[2] single electron transport,[3] and electrical breakdown/peeling of individual tubular layers in a nanotube.[4,5] As nanowire sensors, the conductance of a single wall carbon nanotube has been shown to be affected by external factors such as adsorbed species[6] or mechanical strain.[7,8] These previous works on mechanical deformation of a nanotube were based on using an AFM tip to bend a nanotube lying laterally across contacts. A much more useful configuration is to have a vertical nanotube "tip,"[9–11] as it would allow the implementation of a cantilever-based displacement sensor where one simply pushes against the tip of the nanotube. We show here that as a MWNT bends under a force directed from its tip along the axis, its resistance decreases dramatically. This characteristic is distinctly different to single wall nanotubes for which the resistance increases during bending due to the formation of defects.[7] Thus, the observed drop in resistance during bending must be the result of increasing number of conduction channels in the MWNT and parallel transport through them.

To demonstrate this concept, we prepared individual, vertically aligned MWNTs on a n++-doped Si wafer ($\rho=5\times10^{-3}\ \Omega\,\mathrm{cm}$) by a dc plasma-enhanced chemical vapor (PECVD) deposition technique. High-resolution electron beam lithography was used to pattern the Ni catalyst dots, at the locations where the nanotubes were expected on a TiN layer. The use of TiN as a diffusion barrier layer provided a good electrical contact between the MWNT and the Si substrate[12] at one end [point A of Figs. 1(b) and 1(c)]. The sample used for this study was a square array of 40×40 individual MWNTs, ~5 μm tall and ~60 nm in diameter, at a pitch of 100 μm,[13] ensure that only one nanotube could be contacted by the probe during electrical measurements (Fig. 1(a)).

The electrical contact on the other end of the MWNT [point B of Figs. 1(b) and 1(c)] was obtained by touching the MWNT with a Pt-Ir scanning probe ball having a radius of 100 μm and attached to a five-degree-of-liberty (X,Y,Z,θ,ϕ) piezomanipulator.[14] The probe ball was thermally cleaned *in situ* just before the mechanical contact. The I(V) analyses were done in a vacuum between 10^{-8} to 10^{-9} Torr.

The methodology for assuming and controlling good contact between the CNT and the probe ball is the following. First, the array of nanotubes was scanned from above with the probe ball positively biased at ~200 V. Being high aspect ratio structures, the nanotubes act as tips and field emit when the probe ball was directly above. Hence, it is possible to locate each MWNT by corresponding the measured field emission current with the array spacing.[15] The probe ball was then centered on one MWNT and mechanically contacted by vertically displacing the probe ball.

To control the approach of the probe toward the CNT, we polarized the probe to a few volts. From a certain distance a very fluctuating current turned on, then ending in a

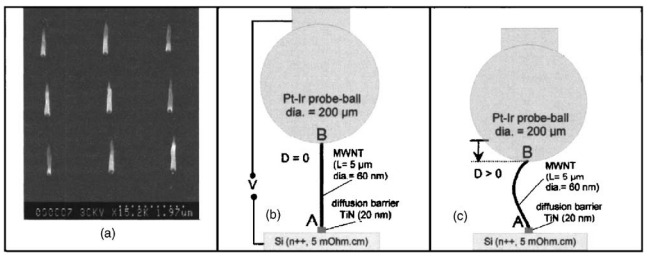

FIG. 1. (a) SEM observation (tilt 20°) of a vertically aligned array of MWNTs (≈5 μm height) grown on a TiN layer with a pitch of 2 μm. In this photo the spacing is 2 μm in order to have on the same photo the array and the MWNTs. (b) and (c) Schematic representations of the experimental setup for $D=0$ (b) and for $D>0$ (c); for the latter case, the MWNT was bent.

[a]Author to whom correspondence should be addressed; electronic mail: vuthien@lpmcn.univ-lyon1.fr
[b]Presently at: LPICM, Ecole Polytechnique, Palaiseau, France.

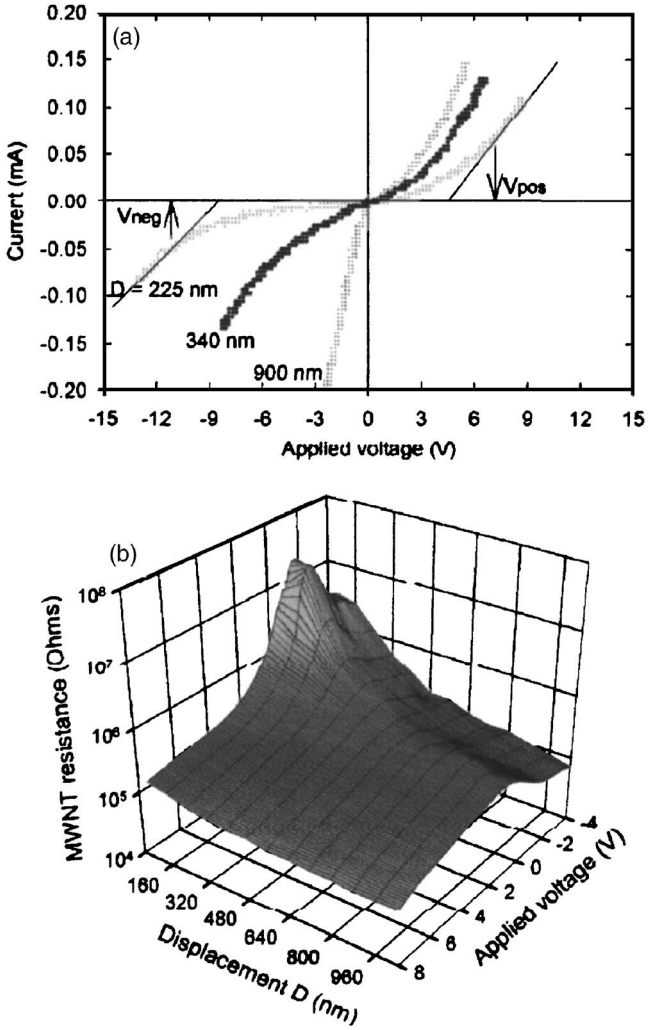

FIG. 2. (a) Current-voltage characteristics presenting a nonlinear conductance for three values of compression, D, for the same nanotube. The distribution of the data points for each of these three plots corresponds to repeated measurements for a fixed D. Note that the plot is limited to only three values of D in order to keep the figure clear. (b) The same data as in (a), but they are plotted to illustrate the variation of the resistance of the MWNT as a function of the applied voltage and for different bending states of $D=80$ to 1040 in steps of $\Delta D=80$ nm. (In this figure all the 13 steps are now represented.)

stable current with a further approach of the probe. We interpret the first step as the appearance of a tunnel current for distances of less than a few nm, and the fluctuations were related to the mechanical vibration of the CNT. We consider the second step as the first contact between the probe and the CNT and it corresponds to $D=0$ of Fig. 1(b). After this initial contact, by pushing the probe ball, for $D>0$, we can deform the nanotube [Fig. 1(c)]. The increase in D, i.e., pushing down the probe ball , was done by steps of ΔD in the range of 100 nm. We assume that there was no lateral displacement of the contact point B between the MWNT and the probe ball (i.e., due to the large dimension of the ball); and second, that this is only a first-order deformation (i.e., arc bending of the nanotube under the mechanical strain). Our second assumption is consistent with experiments of different groups,[16,17] who observed the mechanical deformation of MWNTs by SEM.

To ensure reproducibility, the total current was beyond 1 mA[18] and each $I(V)$ plot presented in Fig. 2 was repeated three to five times. In general, the $I(V)$ characteristics show a "turn-on" behavior in both forward and reverse bias, defined as V_{pos} and V_{neg}, respectively. Beyond these "turn-on" voltages, a practically linear region of $I(V)$ was observed, the resistance of the MWNT can be derived and was in the range of 10^4 to 10^5 Ω over the bending range considered. The observed diode-like behavior of the MWNT is similar to that reported by Yu *et al.*[16] and Li *et al.*[19] As the MWNT is increasingly bent (i.e., increasing D), the resistance [see Fig. 2(b)] and the turn-on voltages (V_{pos} and V_{neg}) decrease. It should also be noted that the turn-on voltages and the resistances observed for $V>0$ and $V<0$ were different, indicating that the MWNT has some electrical anisotropy. The largest mechanical displacement D was ~ 1 μm over a 5 μm tall nanotube—beyond this limit, the nanotube no longer exhibited recoverable/reversible $I(V)$ characteristics.

An immediate reaction to such an $I(V)$ behavior is to question the Ohmic properties of the contacts. As the Pt–Ir probe was thermally cleaned *in situ* just before proceeding to the experiment, we assume then the probe surface to be clean, with metallic properties. Concerning the CNTs, they are obtained by PECVD that favors a tip growth process. Their apexes were then a Ni nanobead covered with graphene layers. By using a simple mechanical model for a stress (σ) versus strain ($\varepsilon=\Delta L/L$) relation, we can estimate σ at the contact point by $\sigma=E\,\varepsilon$, where E is the Young's modulus of the CNT (1 TPa). With ε between 4.5% and 18 %; that means σ between 45 and 180 GPa. These values and the reversibility of all our measurements allow us to consider confidently the probe-CNT contact as a pure resistance R_{S-NT}. The presence of the stress on the axial contact makes it very different from other resistance measurements using the two- or four-probe technique,[20,21] with lateral contacts and no stress.

Finally, let us compare with other resistance values. A given CNT presents the same data for the I(V) characteristics. Different CNTs give different I(V) characteristics, i.e., effective resistance; but all of them show the same behavior and variation, as shown in Fig. 2. For example, the resistance for the highest stress (normalized to 1 μm length) lies between 6 and 16 kΩ/μm. The discrepancies between the different CNTs probably come from the contact, but above all from the intrinsic properties of the CNT itself (dimensions). These values have to be compared to the four-probe measurements (1.4 kΩ/μm$<R<$10.4 kΩ/μm in Ref. 20, and 3.1 kΩ/μm in Ref. 22) or with the suspended structure study (4.2 kΩ/μm of Ref. 18).

The change in resistance as the MWNT bends must therefore be associated with a change in the conduction parameters. Let us assume that there are distinct conduction channels over the tube wall, and these conduction channels only begin to participate in the overall conduction (i.e., "turn-on") when sufficiently large voltages are applied to overcome some barriers. These barriers are lowered under mechanical compression. The reduction in the resistance [the inverse of the slope of the region in Fig. 2(a)] with bending is due to an increase in the number of active channels participating in conduction. According to this model, one would expect to see the reduction in turn-on voltage and resistance as the MWNT is bent. The asymmetry of the turn-on voltages (V_{pos} and V_{neg}) could be due to differences in the properties of the barriers in the two directions.

Thus, an equivalent electrical circuit for the nanotube is a parallel network of channels, each of them having in series

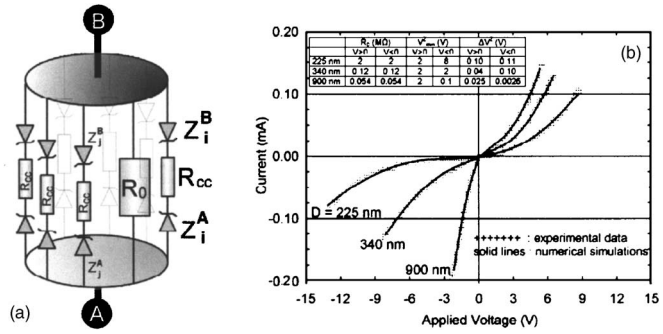

FIG. 3. (a) Equivalent electrical circuit for the nanotube. Each of the elements constituting the parallel network represents one of the conduction channels of the equivalent conduction shell of the nanotube. (b) A comparison between the experimental data (points) and the results from the equivalent electrical circuit simulation (solid lines) for three different bending states (D) of the same MWNT. A value of 3.65 MΩ for R_{CC} gave the best fit, and the evolution in the values of R_0, $V^Z_{\min}$ and ΔV^Z as a function of D are given in the inset table.

one resistance and two opposite Zener diodes (which manifest themselves as the positive and negative turn-on voltages due to the barriers), as shown in Fig. 3(a). Note that in our measurements, the two-terminal resistance R, $R=R_{S-NT}+R_{NT}+R_{NT-B}$, also includes the resistances associated with the substrate-nanotube junction, R_{S-NT}, and the nanotube-probe ball junction, R_{NT-B}. The respective contact resistances R_{S-NT} and R_{NT-B} are estimated to be much less than 1 kΩ, a four-point measurement value of the Ohmic resistance of a MWNT in a stressless contact with a metallic electrode.[23]

To assess this model, we have numerically simulated the electrical behavior of the network of parallel channels, as shown in Fig. 3(a). The following parameters were used to fit the experimental data: a bulk resistance (R_0) that is "on" for all values of V, and a number of conducting channels ("i") with two Zener voltages $V^Z(i)$ with $Z=A,B$ (where A,B denote the positive and negative bias tunnel barriers) and a resistance R_{CC} for each conductive channel. As the voltage across the nanotube is increased for a fixed mechanical strain, each channel will progressively turn-on and conduct due to their different barrier voltages. This behavior can be simply represented by modeling each channel's barrier voltage as $V^Z(i)=V^Z_{\min}+(i\times\Delta V^Z)$.

Here, $V^Z_{\min}$ is the voltage for the first channel, and each channel after has an incrementally larger (ΔV^Z) voltage, thus "turning on" at a higher voltage. Indeed, using this concept, we are able to fit the experimental data for different compressions, as shown in Fig. 3(b). It is clear that as the compression D is increased from 225 to 900 nm, the bulk resistance R_0 falls from 2×10^6 to 5.4×10^4 Ω. Furthermore, we find a decrease in the minimum barrier $V^Z_{\min}$ (for $V<0$, it falls from 8 to 0.1 V) and also a reduction in the ΔV^Z. These simulation-derived data support our postulation that as the nanotube is mechanically compressed, its overall conduction increases as a result of the increasing number of parallel conduction channels that can participate in the overall conduction. However, a detailed and in-depth analysis is still lacking, to associate the electrical model with some solid state physics properties of the CNT, and, in particular, the asymmetry of the I-V behavior.

In conclusion, the experimental data strongly suggest that the MWNT conduction is through a network of parallel channels, each regulated by some barriers that connect the different parts along the nanotubes. By modifying the structure of these junctions with a mechanical strain (bending), one can tune back and forth the number of active conduction channels, and thus modulate the resistance of the nanotubes. As the fabrication technology for single, vertical MWNT is already available,[9–11] this opens up new applications for nanotubes in nanoelectromechanical systems (NEMS), in addition to the proposed approaches,[24] as a nano-displacement sensor based on resistance.

This work was supported by the European Commission (NANOLITH project, IST-1999–11806). K.B.K.T. also acknowledges the support of Christ's College, Cambridge. The authors thank D. G. Hasko and H. Ahmed for the use of the electron beam lithography facilities.

[1] S. Frank, P. Poncharal, Z. L. Wang, and W. A. de Heer, Science **280**, 1744 (1998).
[2] K. Tsukagoshi, B. W. Alphenaar, and H. Ago, Nature **401**, 572 (1999).
[3] M. Bockrath, D. H. Cobden, P. L. McEuen, N. G. Chopra, A. Zettl, A. Thess, and R. E. Smalley, Science **275**, 1922 (1997).
[4] J. Cummings, P. G. Collins, and A. Zettl, Nature **406**, 586 (2000); P. G. Collins, M. Hersam, M. Arnold, R. Martel, and Ph. Avouris, Phys. Rev. Lett. **86**, 3128 (2001).
[5] B. Q. Wei, R. Vajtai, and P. M. Ajayan, Appl. Phys. Lett. **79**, 1172 (2001).
[6] J. Kong, N. R. Franklin, C. Zhou, M. G. Chapline, S. Peng, K. Cho, and H. Dai, Science **287**, 622 (2000).
[7] T. W. Tombler, C. Zhou, L. Alexseyev, J. Kog, H. Dai, L. Liu, C. S. Jayanthi, M. Tang, and S. Y. Wu, Nature **405**, 769 (2000).
[8] S. Paulson, M. R. Falvo, N. Snider, A. Helser, T. Hudson, A. Seeger, R. M. Taylor, R. Superfine, and S. Washburn, Appl. Phys. Lett. **75**, 2936 (1999).
[9] Z. F. Ren, Z. P. Huang, D. Z. Wang, J. G. Wen, J. W. Xu, J. H. Wang, L. E. Calvet, J. Chen, J. F. Klemic, and M. A. Reed, Appl. Phys. Lett. **75**, 1086 (1999).
[10] V. I. Merkulov, D. H. Lowndes, Y. Y. Wei, G. Eres, and E. Voelkl, Appl. Phys. Lett. **76**, 3555 (2000).
[11] K. B. K. Teo, M. Chhowalla, G. A. J. Amaratunga, W. I. Milne, D. G. Hasko, G. Pirio, P. Legagneux, F. Wyczisk, and D. Pribat, Appl. Phys. Lett. **79**, 1534 (2001).
[12] A. M. Rao, D. Jacques, R. C. Haddon, W. Zhu, C. Bower, and S. Jin, Appl. Phys. Lett. **76**, 3813 (2000).
[13] K. B. K. Teo, S. B. Lee, M. Chhowalla, V. Semet, Vu Thien Binh, O. Groening, M. Castignolles, A. Loiseau, G. Pirio, P. Legagneux, D. Pribat, D. G. Hasko, H. Ahmed, G. A. J. Amaratunga, and W. I. Milne, Nanotechnology **14**, 204 (2003).
[14] Vu Thien Binh, V. Semet, J. P. Dupin, and D. Guillot, J. Vac. Sci. Technol. B **19**, 1044 (2001).
[15] V. Semet, Vu Thien Binh, P. Vincent, D. Guillot, K. B. K. Teo, M. Chhowalla, G. A. J. Amaratunga, B. Milne, P. Legagneux, and D. Pribat, Appl. Phys. Lett. **81**, 343 (2002).
[16] M. F. Yu, M. J. Dyer, G. D. Skidmore, H. W. Rohrs, X. K. Lu, K. D. Ausman, J. R. Von Ehr, and R. S. Ruoff, Nanotechnology **10**, 244 (1999).
[17] P. A. Williams, S. J. Papadakis, M. R. Flavo, A. M. Patel, M. Sinclair, A. Seeger, A. Helqser, R. M. Taylor II, S. Washburn and R. Superfine, Appl. Phys. Lett. **80**, 2574 (2002).
[18] S. B. Lee, K. B. K. Teo, M. Chhowalla, D. G. Hasko, G. A. J. Amaratunga, W. I. Milne and H. Ahmed, Microelectron. Eng. **61–62**, 475 (2002).
[19] J. Li, R. Stevens, L. Delzeit, H. T. Ng, A. Cassell, J. Han, and M. Meyyappan, Appl. Phys. Lett. **81**, 910 (2002).
[20] A. Bachtold, M. Henny, C. Terrier, C. Strunk, C. Schonenberger, J. P Salvetat, J. M. Bonard, and L. Forro, Appl. Phys. Lett. **73**, 274 (1998).
[21] J. O. Lee, C. Park, J. J. Kim, J Kim, J. W. Park, and K. H. Yoo, J. Phys. D **33**, 1953 (2000).
[22] L. Zhang, D. Austin, V. I. Merkulov, A. V. Meleshko, K. L. Klein, M. A. Guillorn, D. H. Lowndes, and M. L. Simpson, Appl. Phys. Lett. **84**, 3972 (2004).
[23] Y. F. Hsiou, Y. J. Yang, L. Stobinski, W. Kuo, and C. D. Chen, Appl. Phys. Lett. **84**, 984 (2004).
[24] V. Sazonova, Y. Yaish, H. Ustunel, D. Roundy, T. A. Arias, and P. L. McEuen, Nature **431**, 284 (2004).